MODELING BIOSIGNATURES AROUND HABITABLE WORLDS OBSERVATORY TARGET STARS

University of California, Riverside

Jennifer Park, Edward Schwieterman, Sarah Peacock, Evan Sneed, Wynter Broussard, Margaret Turnbull, Stephen Kane, Breanna Binder

introduction

The abundance and detectability of biosignatures and gases on exoplanets are directly influenced by stellar ultraviolet stellar energy distribution (UV SED). Recent studies have found that the biosignature abundance for gases like CH_4 are enhanced for K-dwarfs, making them favorable targets for direct imaging. As planetary spectrum is highly sensitive to the host star, a full panchromatic spectra of the host star must be used to best accurately analyze biosignatures.

In this project, panchromatic spectra of Habitable Worlds Observatory (HWO) target stars were simulated by the PHOENIX stellar model and input into ATMOS and SMART to explore the biosignatures of Earth-like planets around FGK stars. The PHOENIX model was used to simulate the HWO target spectra based on empirical Chandra or XMM Newton (X ray) and HST NUV + FUV calibration data. The location within the habitable zone (HZ), the atmospheric composition, and climatic conditions are varied to generate comprehensive planetary spectra data.

ATMOS

ATMOS was chosen as the 1D photochemistry-climate code of choice. It includes hundreds of photochemical reactions and vertical transport via eddy diffusion, and solves the continuity and flux equations using a reverse Euler integration method.

1. *Input various FGK stellar panchromatic spectra (121–850 nm) simulated by PHOENIX using empirical data into ATMOS:*
   Sun (G2V), Chi1 Orionis (G0V), Kappa1 Ceti (G5V), GL 620A (G3V), GL 311 (G1V), and GL 892 (K3V)
1. *Vary bulk planetary atmospheric composition:*
   a. *Modern Earth (78% N_2, 21% O_2)*
   b. *Archean Earth (predominantly N_2 with significant CO_2 and CH_4 and little O_2)*
2. *Vary molecular surface fluxes of CH_4, N_2O, and CO from 1×10^{-3} to 10 times modern Earth values (encompassing a plausible range of biological production fluxes)*
3. *Vary location within the HZ to the IHZ, OHZ, and Earth's equivalent flux (F = 1)*
4. *Output: concentrations and chemical profiles for CH_4, N_2O, CO, and O_3, amongst other gases*

Modern Earth Surface Mixing Ratios

	Star Flux Condition	CO	CH_4	N_2O
0	Sun Flux = 1	1.52e-07	1.07e-06	3.39e-07
1	Sun IHZ	1.37e-07	9.49e-07	3.28e-07
2	Sun OHZ	5.43e-07	4.42e-06	4.84e-07
3	Chi Ori Flux = 1	1.34e-07	9.29e-07	3.13e-07
4	Chi Ori IHZ	1.20e-07	8.07e-07	3.03e-07
5	Chi Ori OHZ	4.46e-07	3.60e-06	4.27e-07
6	Kap Ceti Flux = 1	1.97e-07	1.48e-06	4.55e-07
7	Kap Ceti IHZ	1.78e-07	1.31e-06	4.37e-07
8	Kap Ceti OHZ	8.07e-07	6.66e-06	7.66e-07
9	GL620 Flux = 1	1.76e-07	1.29e-06	3.39e-07
10	GL620 IHZ	1.56e-07	1.11e-06	3.28e-07
11	GL620 OHZ	6.45e-07	5.27e-06	4.80e-07
12	GL311 Flux = 1	1.64e-07	1.17e-06	3.12e-07
13	GL311 IHZ	1.45e-07	1.01e-06	3.03e-07
14	GL311 OHZ	5.73e-07	4.66e-06	4.12e-07
15	GL892 Flux = 1	5.48e-07	4.56e-06	1.00e-06
16	GL892 IHZ	5.57e-07	4.64e-06	1.00e-06
17	GL892 OHZ	4.15e-06	3.13e-05	2.37e-06

Archean Earth Surface Mixing Ratios

	Star Flux Condition	CO	CH_4
0	Sun Flux = 1	1.49e-05	5.42e-04
1	Sun IHZ	1.17e-05	4.34e-04
2	Sun OHZ	2.80e-05	1.75e-02
3	Chi Ori Flux = 1	3.43e-06	1.50e-04
4	Chi Ori IHZ	2.58e-06	1.17e-04
5	Chi Ori OHZ	3.26e-05	1.31e-03
6	Kap Ceti Flux = 1	4.93e-05	3.23e-03
7	Kap Ceti IHZ	5.56e-05	2.48e-03
8	Kap Ceti OHZ	2.84e-05	1.66e-02
9	GL620 Flux = 1	1.07e-05	3.84e-04
10	GL620 IHZ	8.21e-06	3.11e-04
11	GL620 OHZ	4.55e-05	4.58e-03
12	GL311 Flux = 1	9.98e-07	5.86e-05
13	GL311 IHZ	8.56e-07	5.10e-05
14	GL311 OHZ	1.03e-05	4.30e-04
15	GL892 Flux = 1	1.01e-06	5.90e-05
16	GL892 IHZ	1.03e-06	5.98e-05
17	GL892 OHZ	3.40e-05	9.21e-04

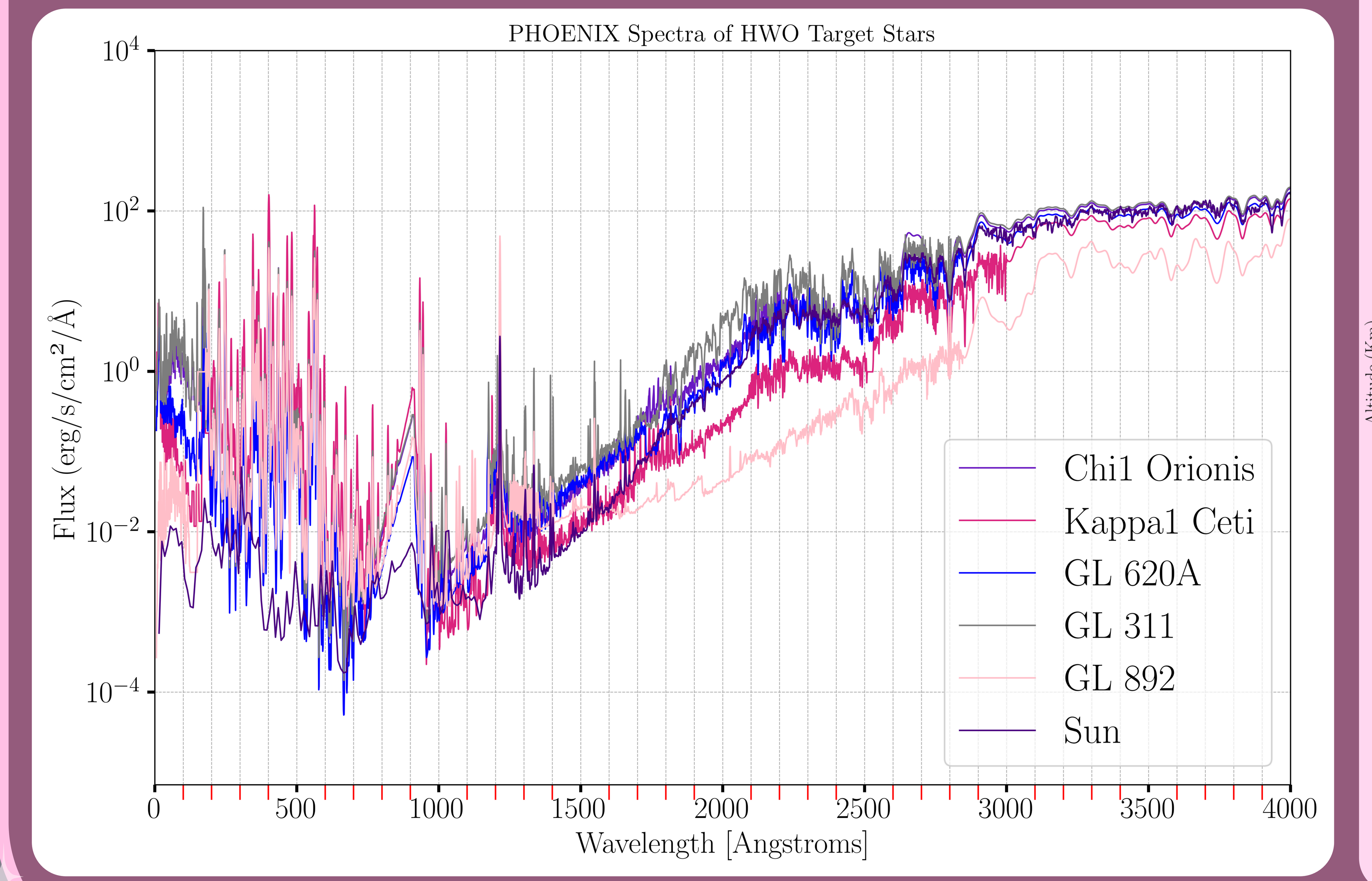

SMART

SMART is a line-by-line, fully multiple scattering radiative transfer model used to generate UV-VIS-NIR-MIR planetary spectra from 0.2–2.5 μm mimic optimistic potential HWO capabilities.

1. *Input concentration and chemical profiles of biosignature gases under Modern Earth/Archean Earth atmosphere from ATMOS*
2. *Input HITRAN 2020 line lists*
3. *Implement partial cloud-cover (50% clouds, half liquid and half cirrus) + a weighted surface spectral albedo (~66% ocean and 34% land surfaces which is a mix of soil, snow/ice, and vegetation)*
4. *These spectra are simulated for systems that will be directly imageable by telescopes like HWO*

We focus on comparing the CH_4 levels between the Sun and GL 892 (OHZ) for Modern Earth atmosphere due to high differences in CH_4 abundances.

Spectra combining clear sky + clouds for Modern Earth atmosphere

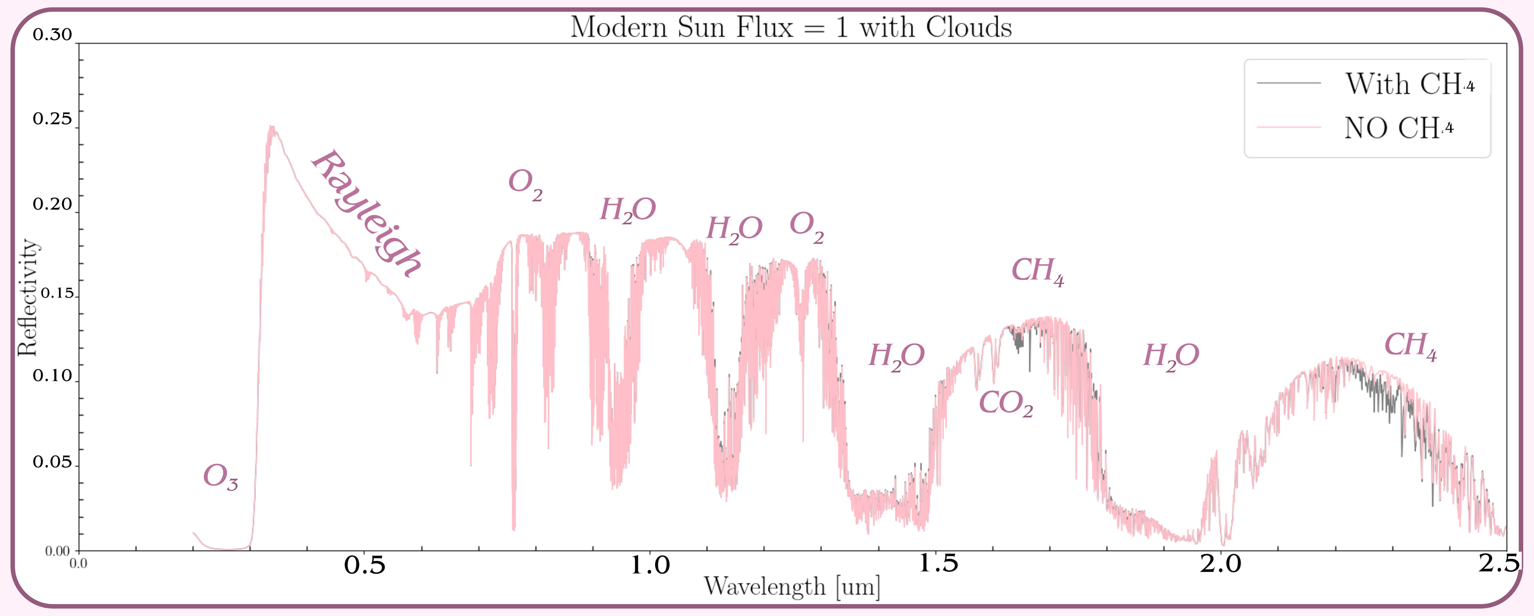

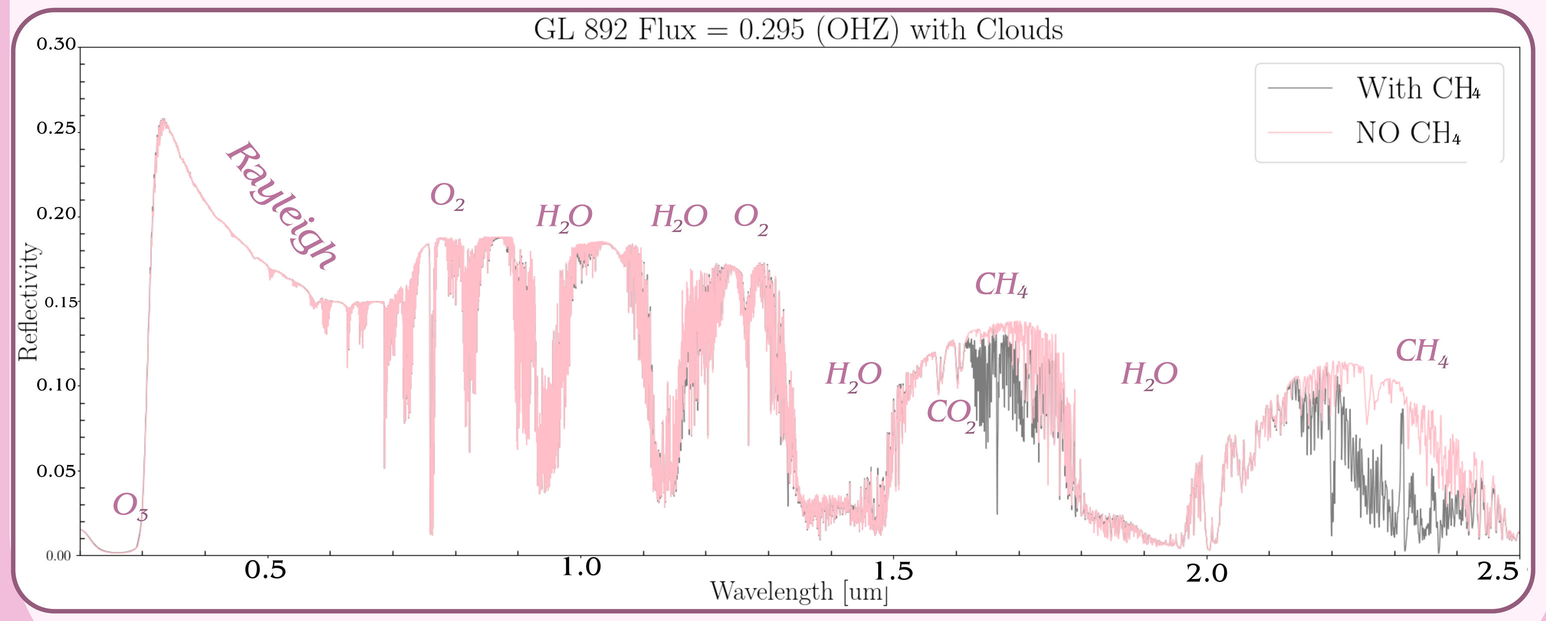

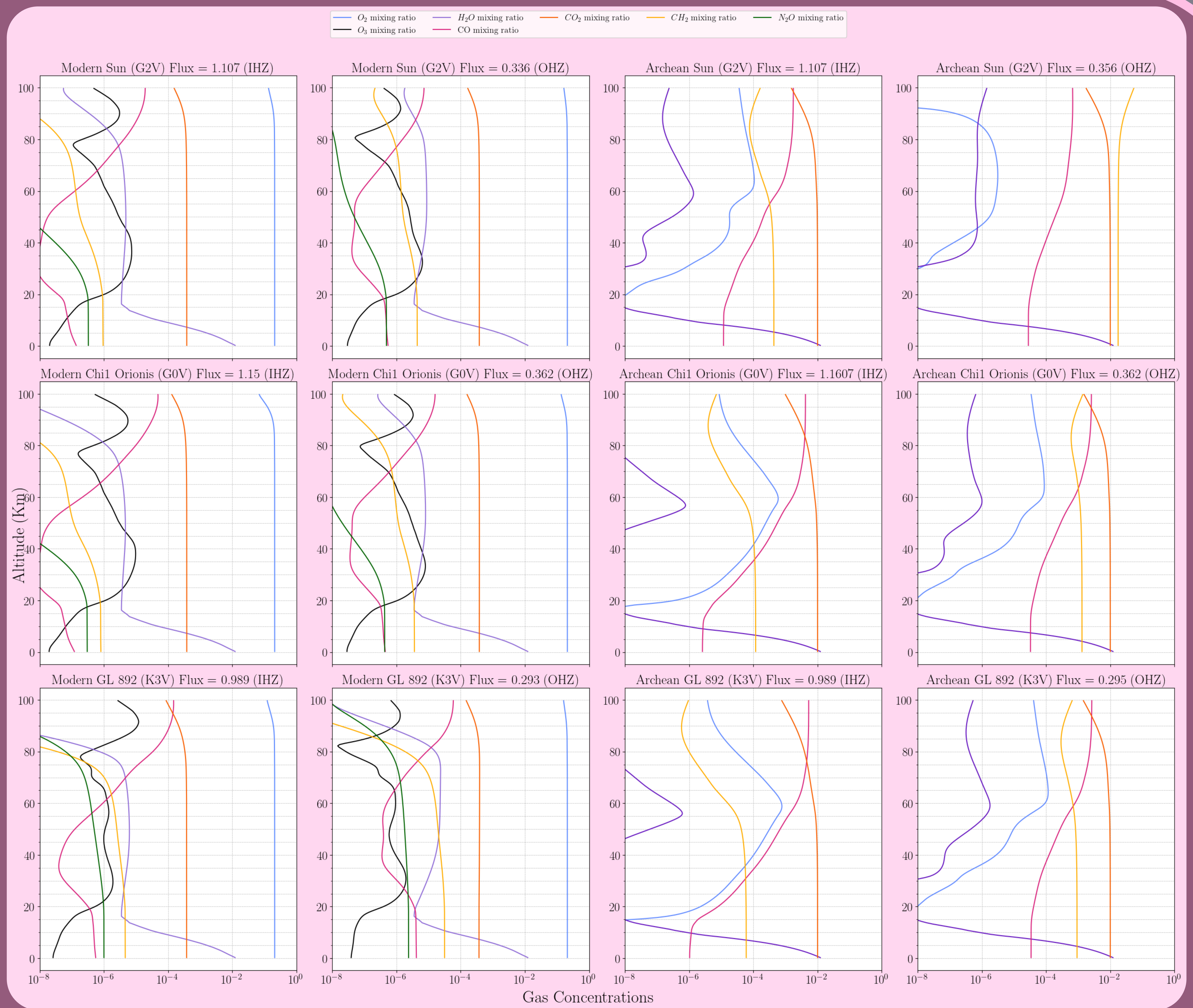

Gas Concentrations for the Earth and Archean Earth Cases

preliminary results

The simultaneous presence of methane and molecular oxygen within an atmosphere is a compelling potential planetary biosignature. Typically, methane and oxygen should exist in a non-detectable equilibrium due to their high reactivity and efficient destruction via photochemistry and geochemical processes (with products H_2O and CO_2). However, on Earth, both methane and oxygen exist in thermodynamic and chemical disequilibrium—both are continuously replenished by robust biological processes, making their coexistence a significant biosignature. However, the photochemical destruction rate of methane is highly dependent on the host star's ultraviolet radiation output, particularly the flux of near-UV radiation that can penetrate to the lower atmosphere. A planet orbiting a K dwarf star can maintain an order of magnitude more methane than when orbiting a G dwarf star due to lower NUV output (Arney et al. 2019), a consequence of its lower temperature photosphere. Additionally, lower NUV can result from a planet residing farther out in its habitable zone. These joint contributing factors are evident in the comparing the predicted methane levels between an Earth-twin orbiting the Sun (G2V) and GL 892 (K3V). Thus, O_2-CH_4 disequilibrium is potentially most favorably observed in direct imaging observations of planets within the mid-outer HZs of K dwarfs, which will benefit from the following favorable factors: (1) greater abundance of K dwarf target stars, (2) better contrast ratios than for G or F dwarfs, (3) more favorable IWAs for outer-HZ targets, and (4) more favorable conditions for the photochemical accumulation of CH_4 in O_2-rich and O_2-poor atmospheres (the subject of this poster).

future work

The next steps are to extend the spectral analysis to the remaining FGK stars. This involves running SMART for each star under both the Modern and Archean Earth cases. This is vital in interpreting how different star types influence atmospheres and surface processes on exoplanets, as well as providing predictions for the potential accumulation and detectability of biosignature gases in various systems, which could help prioritize those targets for future mission like HWO.

Citations:

Gaudi et al. (2020). "The Habitable Exoplanet Observatory (HabEx) Mission Concept Study Final Report". arXiv: 2001.06683 (astro-ph.IM).

Marais et al. (2002). "Remote Sensing of Planetary Properties and Biosignatures on Extrasolar Terrestrial Planets". Astrobiology 2.2, pp. 153–181. doi: 10.1089/15311070260192246.

NASA Exoplanet Science Institute (2023). NASA ExEP Target List for the Habitable Worlds Observatory: Documentation. NASA Exoplanet Archive.

Rugheimer et al. (2015). "Effect of UV Radiation on the Spectral Fingerprints of Earth-like Planets Orbiting M Stars". The Astrophysical Journal 809.1, p. 57. doi: 10.1088/0004 637X/809/1/57. arXiv: 1506.07202.

Schwieterman and Leung (2024). "An Overview of Exoplanet Biosignatures". arXiv: 2404. 15431 (astro-ph.EP).

Arney, G. N. (2019). "The K Dwarf Advantage for Biosignatures on Directly Imaged Exoplanets" The Astrophysical Journal Letters, Volume 873, Number 1. doi: 10.3847/2041-8213/ab0651

Young, Amber V. (2025). "Modern Earth-like Chemical Disequilibrium Biosignatures are Challenging to Constrain through Spectroscopic Retrievals". The Astrophysical Journal, Volume 986, Number 2. doi: 10.3847/1538-4357/addbd7